Mechanisms causing thermal rectification: The influence of phonon frequency, asymmetry, and nonlinear interactions

Nan Zeng*
Department of Physics, National University of Singapore, Singapore 117542, Republic of Singapore and CSIRO Materials Science and Engineering, P.O. Box 218, Lindfield, New South Wales 2070, Australia

Jian-Sheng Wang
Center for Computational Science and Engineering and Department of Physics, National University of Singapore, Singapore 117542, Republic of Singapore

(Received 16 April 2008; published 30 July 2008)

We have determined the mechanisms leading to thermal rectification by applying the nonequilibrium Green's function method to study thermal transport through a one-dimensional asymmetric lattice. Thermal rectification occurs in the presence of nonlinear interactions and a nonuniform phonon frequency distribution. We show that thermal rectification results from the contribution of high-frequency phonons; a thermal rectifier can thus be realized by filtering out high-frequency phonons in a single direction. Using these results, we present methods of increasing the level of rectification, and also discuss possible limitations on thermal rectifier performance.

DOI: 10.1103/PhysRevB.78.024305 PACS number(s): 63.20.kg, 44.10.+i, 63.20.Ry, 63.22.−m

I. INTRODUCTION

Although its counterpart in electronics was invented a hundred years ago, the exciting possibility of a thermal rectifier is only now becoming a reality as a result of progress in nanotechnology. The novel electrical and thermal properties of nanoscale systems make them good candidates for solid-state thermal rectifiers. However, to design and optimize useful thermal rectifiers, it is essential to gain an understanding of the fundamental mechanisms behind thermal rectification. Previous work, reviewed below, has shown that two conditions are necessary. The first is that the system must be asymmetric. The second is that there must be nonlinear interactions in the system. While the first condition is obvious, the mechanisms by which the second comes into play are poorly understood.

In this paper we present results that give a clear understanding of how thermal rectification arises from the interplay of asymmetry of the structure and nonlinear interactions. We obtain these important insights by applying the powerful nonequilibrium Green's function method to study the thermal conductance through a one-dimensional (1-D) asymmetric lattice. In particular, this method allows us to determine the frequency dependence of the phonon transmission through the lattice. As a consequence, we are able to determine how to increase the thermal rectification ratio, and to understand limitations on thermal rectifier performance.

The observation of thermal rectification effect dates back to the 1930s when Starr[1] studied the thermal conductance of the copper oxide rectifier. A series of experiments[2–7] had been investigated after Barzelay *et al.*[8] noted that there was a directional effect for heat transfer at the interface of dissimilar metals. However, these experiments did not lead to the realization of an applicable thermal rectifier due to the complex requirements at the metal-metal interface and lack of theoretical support. In the last decade, thermal transport in nanoscale systems has gained a lot of attention and the number of theoretical studies on such issues are booming,[9] including works on thermal rectification effect. Terraneo *et al.*[10] suggested a possible one-dimensional thermal rectifier model using molecular dynamics simulations. Their model consisted of a chain of particles with harmonic coupling and a Morse on-site potential giving rise to nonlinear interactions. The thermal rectification effect was observed with asymmetrical chain structure using different parameters of the Morse function. A different model that showed thermal rectification effect was constructed with two separate nonlinear lattices connected by a harmonic link.[11–17] Experiments to measure the thermal conductance of nanowires began to appear in recent years.[18,19] An experiment measuring the thermal conductance of a nanotube with a coating of increasing mass along the length of the nanotube was carried out by Chang *et al.*,[18] which is the first of this kind. It was noted that thermal flux transmits better in the direction of mass decrement, which cannot be explained by the wave theory, and the authors claimed that the observed rectification should be related to solitons. A follow-up study by Yang *et al.*[20] with a simple one-dimensional model confirmed the rectification effect in such a structure. However, their explanation did not answer the question why nonlinear interactions are important for thermal rectification. Simulations to look for thermal rectification in a more complicated nanotube were also carried out.[21] While most of the results were obtained from classical molecular dynamics simulations, we also note the work of Segal and Nitzan[22–24] in which a two level system was analyzed quantum mechanically, and in which thermal rectification was also found.

II. METHOD

Our model is a one-dimensional system which is separated into three sections. The right and left sections are semi-infinite linear leads that act as heat baths. The central junction section is coupled to the leads through linear interactions. It can have any structure and it also includes nonlinear interactions. The Hamiltonian of the total system is

 ©2008 The American Physical Society

$$\mathcal{H} = \sum_{\alpha=L,C,R} H_\alpha + u_L^T V_{LC} u_C + u_C^T V_{CR} u_R + H_n, \tag{1}$$

where

$$H_\alpha = \sum_i \frac{1}{2}\dot{u}_{\alpha i}^2 + \sum_{ij} \frac{1}{2} k_{\alpha,ij} u_{\alpha i} u_{\alpha j}$$

is the harmonic Hamiltonian of each section,

$$H_n = \sum_{ijk} \frac{1}{3} k_{ijk} u_{Ci} u_{Cj} u_{Ck} + \sum_{ijk} \frac{1}{4} k_{ijkl} u_{Ci} u_{Cj} u_{Ck} u_{Cl}$$

describes the nonlinear interaction in the junction region, u_α with $\alpha=L,C,R$ is the normalized displacement vector of each section with component $u_{\alpha i}=x_{\alpha i}\sqrt{m_{\alpha i}}$ of each atom i, V_{LC} and V_{CR} are the interactions between the junction and the left and right leads, respectively, $k_{\alpha,ij}$ is the second-order interaction coefficient between two atoms in each section, and k_{ijk} and k_{ijkl} are the third- and fourth-order nonlinear interaction coefficients in the junction section, respectively.

In order to obtain the thermal conductance of the system, we need to know the thermal flux first, which is defined as the rate of the energy flow from the lead to the junction. Thus the flux out of the left lead is

$$J_L = -\langle \dot{H}_L(t) \rangle, \tag{2}$$

where $\langle\ \rangle$ stands for the average over the density matrix at steady state.[25] Because the energy must be conserved, the thermal flux from the left lead should equal the flux entering the right lead, which yields $J_R=-J_L$. The thermal flux can be written in a symmetrical form as

$$J = \frac{1}{4}(J_L + J_L^* - J_R - J_R^*), \tag{3}$$

where the $*$ represents the quantity's complex conjugate. The contour-ordered Green's function used in our calculation is defined as

$$G^{\alpha\beta}(\tau,\tau') \equiv -i\langle \mathcal{T}_c u^\alpha(\tau) u^\beta(\tau')^T \rangle, \tag{4}$$

where α and β refer to the section that the coordinates belong to and $\mathcal{T}_c$ is the contour-ordering operator. The thermal flux Eq. (3) can be represented by Green's functions as

$$J = \frac{1}{4\pi}\int_0^\infty \omega\ \mathrm{Tr}[(G^r - G^a)(\Sigma_R^< - \Sigma_L^<) + iG^<(\Gamma_R - \Gamma_L)]d\omega, \tag{5}$$

where $G^<$ stands for the abbreviation of $G^<(\tau,\tau') = -i\langle u(\tau')u(\tau)^T\rangle^T$ with $\tau<\tau'$, G^r and G^a are retarded and advanced Green's functions defined as

$$G^r(\tau,\tau') = -i\theta(\tau-\tau')\langle [u(\tau), u(\tau')^T]\rangle,$$

$$G^a(\tau,\tau') = i\theta(\tau'-\tau)\langle [u(\tau), u(\tau')^T]\rangle,$$

respectively, $\Sigma_\alpha = V_{C\alpha} g_\alpha V_{\alpha C}$ is the self-energy due to interaction with the heat bath and $\Gamma_\alpha = i(\Sigma_\alpha^r - \Sigma_\alpha^a)$. The thermal conductance can now be calculated from the thermal flux by differentiating with respect to the temperature difference between the heat baths, i.e.,

$$\kappa = \lim_{\Delta T\to 0} \frac{J}{\Delta T}. \tag{6}$$

For ballistic electronic transport, the conductance can be calculated using the Landauer formula. For thermal transport with nonlinear interactions, we can obtain a similar formula by defining an effective transmission function.[25] Writing Eq. (6) in the Landauer form, we have

$$\kappa = \frac{1}{2\pi}\int_0^\infty \omega T(\omega) \frac{\partial f(\omega)}{\partial T} d\omega, \tag{7}$$

where $T(\omega)$ is an effective transmission function and represents the probability of a phonon with frequency ω transmitting from one side of the junction to the other side, and $f(\omega)=(e^{\hbar\omega/kT}-1)^{-1}$ is the Bose-Einstein distribution.

III. THERMAL RECTIFICATION IN 1-D CHAIN WITH VARYING MASS

We numerically calculated the thermal conductance and the effective transmission function of a one-dimensional chain model with an uneven mass distribution in the junction section. Mean-field approximation was utilized in the calculation of the self-energy. The model is similar to Ref. 20, which has been studied using molecular dynamics method. H_α and H_n of this specific model are

$$H_\alpha = \sum_i \frac{1}{2}\dot{u}_{\alpha i}^2 + \sum_{i,j=i\pm1} \frac{1}{2} k_{\alpha,ij}(u_{\alpha i} - u_{\alpha j})^2,$$

$$H_n = \sum_{i,j=i\pm1} \frac{1}{3} k_{3,ij}(u_{Ci} - u_{Cj})^3 + \sum_{i,j=i\pm1} \frac{1}{4} k_{4,ij}(u_{Ci} - u_{Cj})^4.$$

The tight-binding approximation is assumed here, so that each atom only interacts with its two nearest neighbors. The interaction coefficients between adjacent atoms are obtained from the Morse potential $D\{\exp[a(r-r_0)^2]-1\}^2$, where $D=70$ kcal/mol, $a=\sqrt{5}$ Å^{-1}, and r_0 is the equilibrium distance between adjacent atoms. The values of these parameters were obtained from Ref. 26 for C-C interactions. The third- and fourth-order coefficients are obtained by Taylor expansion of the potential around the equilibrium distance. The left lead and the right lead maintain a temperature difference ΔT, which gives $T_L=T+\Delta T/2$ and $T_R=T-\Delta T/2$ for a particular temperature T, or in the reverse order for heat flows in the opposite direction.

In the following part, without specification, the unit of mass is g/mol, the units of the second-, third- and fourth-order interaction coefficients are eV/Å^2, eV/Å^3 and eV/Å^4, respectively, and the unit of temperature is K as usual. All other quantities have units derived from these.

The junction section is comprised of 20 atoms. The mass of each atom is $m_p=m_L(1+0.4p)$ with $p\in[0,20)$. The second-order force constant between adjacent atoms is $k_2=17.3$. The third and fourth interaction coefficients are $k_3=-116$ and $k_4=605.6$, respectively. This setup is similar to

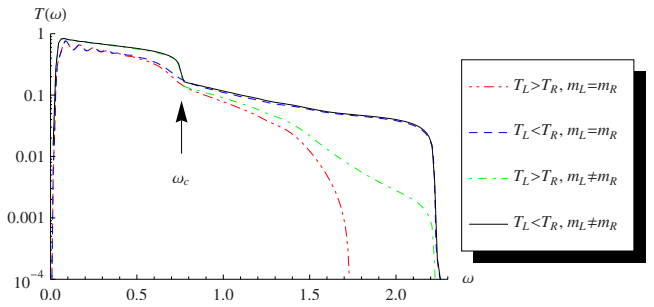

FIG. 1. (Color online) Effective thermal transmission vs phonon frequency, with $n=20$, $m_p=m_L(1+0.4p)$ in the junction region. The dot-dot-dashed line and the dashed line have the same heat baths at each end with $m_L=m_R=14$. The dot-dashed line and the solid line have different heat baths at each end with $m_L=14$ and $m_R=120.4$. ω_c is the separation frequency of the high-frequency region and the low-frequency region.

the experimental conditions for which thermal rectification was measured on a nanotube coated unevenly with heavy molecules.[18] The mass gradient provides the necessary asymmetrical structure for thermal rectification, and three-body and four-body interactions are included to fulfill the requirement of nonlinear interactions.

The thermal transmission probability $T(\omega)$ of phonons with different frequencies is shown in Fig. 1. The dot-dot-dashed line represents the result for thermal flux flow from left to right with temperature $T_L=1100$ and $T_R=900$. The dashed line shows the results when the direction of thermal flux is reversed. The heat baths at both ends of the junction are identical with a monatomic lattice basis of mass $m_L=m_R=14$. The plot is divided into two regions by frequency ω_c. From Fig. 1 we notice that at low frequencies, where $\omega<\omega_c$, the transmission probability difference between the two curves is small, while at high-frequency region, where $\omega>\omega_c$, the difference is quite noticeable. This indicates that the thermal rectification effect is due to the contribution of high-frequency phonons.

To examine the effect of heat baths on the transmission probability, we change the lattice basis mass of the right heat bath to $m_R=120.4$ to match the right end of the junction. The results are shown by the solid line and the dot-dashed line in Fig. 1. This time, the separation of the low-frequency region and the high-frequency region is more obvious. In fact, the separation frequency ω_c is approximately equal to $\sqrt{4k_2/M_{\max}}$ where $M_{\max}$ is the maximum atom mass in the chain, and yields $\omega_c=0.758$. When $\omega>\omega_c$, we notice that the $T(\omega)$s for phonons flowing from right to left match almost exactly in both heat bath setups. This means that the change of the right heat bath does not affect the transmission probability of phonons flowing into the right side. In both cases, there are thermal transmission differences for phonons flowing in opposite directions, thus this difference must be related to the asymmetry of the central junction section.

IV. ASYMMETRY AND NONLINEAR INTERACTIONS

Asymmetry is an essential feature of systems with thermal rectification effect. This can be explained by considering the

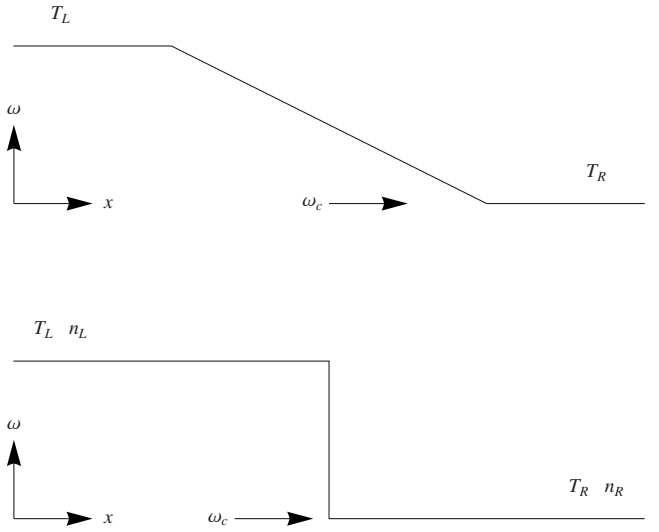

FIG. 2. Maximum transmittable phonon frequencies for a one-dimensional chain with mass varying junction section connected with different heat baths (upper) and a simplified version (lower).

phonon frequency distribution across the system. Because of the asymmetrical structure of the system, the maximum phonon frequency is not uniformly distributed. A schematic view of this distribution corresponding to the model in Sec. III is shown in the upper part of Fig. 2. The maximum phonon frequency decreases gradually from one end of the junction section to the other end due to the variation of the atom mass. The heat baths connected to the junction have different atom mass for generality. This plot can be further simplified to a stair figure as shown in the lower part of Fig. 2.

In this simplified picture, two sections are connected together. Each of them is in an equilibrium state with its own specific temperature noted by T_L and T_R, respectively. The left side has higher frequency phonons compared with the right side, and these higher frequency phonons cannot enter the right side due to the blocking at the interface. The thermal flux through the interface can be expressed as the sum of energy carried by phonons of different modes, i.e.,

$$\mathbf{J}=\sum_k (n_k^L-n_k^R)\hbar\omega_k\mathbf{v}, \tag{8}$$

where $n_k^{L,R}$ is the phonon occupation number of mode k in each section, $\mathbf{v}$ is the phonon group velocity, and $\hbar\omega$ is the individual phonon energy.

When $T_L=T_R$, the occupation numbers of lower frequency phonons on both sides of the interface are equal, thus there is no net thermal flux flowing through the interface. When $T_L\neq T_R$, the nonzero phonon occupation number difference incurs a thermal flux. In the case $T_L>T_R$, as phonons with frequencies $\omega>\omega_c$ are blocked at the interface, only phonons with $\omega\leq\omega_c$ contribute to the thermal flux. The total thermal flux is

$$J=\sum_{\omega\leq\omega_c}[n_L(\omega)-n_R(\omega)]\hbar\omega\mathbf{v}. \tag{9}$$

On the other hand, if $T_L<T_R$, the thermal flux direction is reversed. Because of the existence of nonlinear interactions,

some phonons with lower frequencies will be scattered through normal and umklapp processes to higher frequencies. This mechanism provides an additional flux channel with carriers of higher frequencies. For the low-frequency phonons, this loss of phonon density due to the conversion will be compensated by allowing more phonons to enter the interface from the right side, so that eventually the same occupation number difference as Eq. (9) is achieved for low-frequency phonons at steady state. The total thermal flux is thus the sum of the flux carried by high-frequency phonons and that carried by low-frequency phonons. This is the reason why the thermal conductance is larger when the thermal flux flows from a region with lower upper limit frequency to a region with higher upper limit frequency. In the case of junctions with varying mass, the thermal conductance is larger in the mass decreasing direction. This conclusion is in agreement with Ref. 18.

It should be emphasized that nonlinear interactions play an essential role in thermal rectification. Without them, there is no conversion between different phonon modes, thus high-frequency phonons would not contribute to the thermal transport, and no thermal rectification effect would exist.

V. THERMAL RECTIFICATION RATIO

The discussion in Sec. IV provides a proper way to define the thermal rectification ratio, which signifies the effectiveness of the system's thermal rectification property. We define the thermal rectification ratio as the thermal conductance of high-frequency phonons with $\omega > \omega_c$ divided by the sum of the thermal conductance of low-frequency phonons and high-frequency phonons, which is equal to the absolute value of the thermal conductance difference in opposite directions divided by the maximum thermal conductance in both directions, i.e.,

$$\gamma = \frac{\kappa(\omega > \omega_c)}{\kappa(\omega > \omega_c) + \kappa(\omega \leq \omega_c)} = \frac{|\kappa_{L\to R} - \kappa_{R\to L}|}{\mathrm{MAX}(\kappa_{L\to R}, \kappa_{R\to L})}, \tag{10}$$

where $\kappa_{L\to R}$ is the thermal conductance for heat flows from left to right and $\kappa_{R\to L}$ is the thermal conductance in the opposite direction. This definition yields $\gamma=0$ for symmetric thermal transport and $0<\gamma<1$ for asymmetric thermal transport.

As the proportion of high-frequency phonons in the overall heat carriers determines the efficiency of thermal rectification, we should look for ways to maximize it to gain a higher thermal rectification ratio. One possible method is to adjust the separation frequency ω_c so that heat carried by low-frequency phonons is reduced. In other words, the separation frequency ω_c needs to be as small as possible. Figure 3 shows the dependence of thermal rectification ratio γ on the heat bath mass ratio. The atoms in the junction section have mass $m_p=m_L=14$, and the atoms in the right lead have mass $m_R=\beta m_L$ with β ranging from 2 to 1024. In actual experiments, a big value of β can be realized by attaching heavy organic molecules to a linear polymer chain or other linear-chain structures properly. The right lead behaves like a high-frequency phonon filter, with only low-frequency phonons allowed to enter. The interaction coefficients are chosen as previously, i.e., $k_2=17.3$, $k_3=-116$, and $k_4=605.6$. Figure 3 shows that as β increases, the thermal rectification ratio γ increases too. The inset of Fig. 3 shows the dependence of the thermal conductance difference $\Delta\kappa$ on β. $\Delta\kappa$ becomes a constant when β is sufficiently large. The low-frequency phonons are effectively suppressed, which means that the major contribution to the thermal conductance comes from the high-frequency phonons. However, it should also be pointed out that even though the rectification ratio can be increased due to the reduced weight of low-frequency phonons in the conduction, the actual thermal flux can be rather small. This is caused by the low density of high-frequency phonons generated in the junction section.

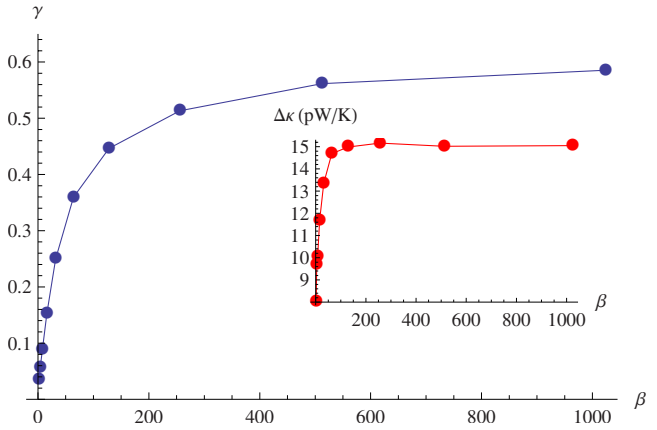

FIG. 3. (Color online) Thermal rectification ratio γ vs heat bath mass ratio $\beta=m_R/m_L$. The inset gives the dependence of the thermal conductance on β for opposite flow directions.

In order to increase the number of high-frequency phonons in the junction, we recall that this is temperature related. When the temperature gets higher, more phonons are generated, so the chance of collision is also increased. The relation between the thermal rectification ratio γ and the temperature is illustrated in Fig. 4, with the same model parameters as in Fig. 3 and with β set to 512. Figure 4 shows that the thermal rectification ratio increases as the temperature is raised.

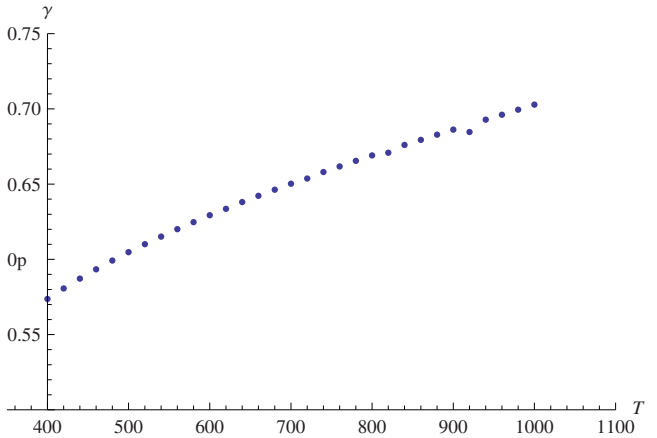

FIG. 4. (Color online) Temperature dependence of thermal rectification ratio with $m_L=14$, $m_R=\beta m_L$, $\beta=512$, and $n=20$.

VI. CONCLUSION

In conclusion, we have discussed the thermal rectification effect in a one-dimensional asymmetrical lattice with nonlinear interactions using the nonequilibrium Green's function method. This allowed us to calculate the effective thermal transmission function for phonons. We have shown that thermal rectification is caused by the transmission of high-frequency phonons. These high-frequency phonons are generated from low-frequency phonons by collisions. A thermal rectifier can be realized by designing an effective high-frequency phonon filter at one end of the system so that heat carried by high-frequency phonons are forbidden to enter at one end but freely transmittable at the other end. The thermal rectification ratio can be effectively increased by reducing the weight of low-frequency phonons in the entire phonon spectrum. On the other hand, the thermal flux across the system is limited by the conversion rate between low-frequency phonons and high-frequency phonons.

ACKNOWLEDGMENTS

The authors thank Jingtao Lü, Jian Wang, Anthony B. Murphy and Karl-Heinz Müller for discussions. This work was supported in part by a Faculty Research Grant of National University of Singapore.

*zengnan@gmail.com

[1] C. Starr, Physics (N.Y.) **7**, 15 (1936).
[2] G. F. C. Rogers, Int. J. Heat Mass Transfer **2**, 150 (1961).
[3] A. M. Clausing, Int. J. Heat Mass Transfer **9**, 791 (1966).
[4] D. V. Lewis and H. C. Perkins, Int. J. Heat Mass Transfer **11**, 1371 (1968).
[5] P. W. O'Callaghan, S. D. Probert, and A. Jones, J. Phys. D **3**, 1352 (1970).
[6] T. R. Thomas and S. D. Probert, Int. J. Heat Mass Transfer **13**, 789 (1970).
[7] R. W. Powell, R. P. Tye, and B. W. Jolliffe, Int. J. Heat Mass Transfer **5**, 897 (1962).
[8] M. Barzelay, K. Tong, and G. Holloway, NACA Report No. TN-3295, 1955 (unpublished).
[9] J.-S. Wang, J. Wang, and J. T. Lu, Eur. Phys. J. B **62**, 381 (2008).
[10] M. Terraneo, M. Peyrard, and G. Casati, Phys. Rev. Lett. **88**, 094302 (2002).
[11] B. Li, L. Wang, and G. Casati, Phys. Rev. Lett. **93**, 184301 (2004).
[12] B. Li, J. Lan, and L. Wang, Phys. Rev. Lett. **95**, 104302 (2005).
[13] J. Lan and B. Li, Phys. Rev. B **74**, 214305 (2006).
[14] B. Hu and L. Yang, Chaos **15**, 015119 (2005).
[15] B. Hu, L. Yang, and Y. Zhang, Phys. Rev. Lett. **97**, 124302 (2006).
[16] B. Hu, D. He, L. Yang, and Y. Zhang, Phys. Rev. E **74**, 060101(R) (2006).
[17] J. Lan and B. Li, Phys. Rev. B **75**, 214302 (2007).
[18] C. W. Chang, D. Okawa, A. Majumdar, and A. Zettl, Science **314**, 1121 (2006).
[19] Z. Wang, J. A. Carter, A. Lagutchev, Y. K. Koh, N.-H. Seong, D. G. Cahill, and D. D. Dlott, Science **317**, 787 (2007).
[20] N. Yang, N. Li, L. Wang, and B. Li, Phys. Rev. B **76**, 020301(R) (2007).
[21] G. Wu and B. Li, Phys. Rev. B **76**, 085424 (2007).
[22] D. Segal and A. Nitzan, Phys. Rev. Lett. **94**, 034301 (2005).
[23] D. Segal and A. Nitzan, J. Chem. Phys. **122**, 194704 (2005).
[24] D. Segal, Phys. Rev. B **73**, 205415 (2006).
[25] J.-S. Wang, N. Zeng, J. Wang, and C. K. Gan, Phys. Rev. E **75**, 061128 (2007).
[26] S. L. Mayo, B. D. Olafson, and W. A. Goddard III, J. Phys. Chem. **94**, 8897 (1990).